

Quantum simulation of thermodynamics: Maxwell relations for pair correlations

F. Rist,¹ R. S. Watson,¹ H. L. Nourse,² B. J. Powell,^{1,*} and K. V. Kheruntsyan^{1,†}

¹*School of Mathematics and Physics, University of Queensland, Brisbane, Queensland 4072, Australia*

²*School of Chemistry, University of Sydney, Sydney, NSW 2006, Australia*

(Dated: June 25, 2025)

Quantum simulators hold enormous promise for advancing the modelling of materials and understanding emergent physics, such as high temperature superconductivity and topological order. While correlation functions are, typically, straightforward to measure in quantum simulators, thermodynamic properties are not. This limits our ability to directly compare the results of quantum simulations to experiments on the materials being modelled. Maxwell relations are an extremely powerful tool for characterising complex materials, as they enable the determination of challenging-to-measure thermodynamic properties from more accessible ones. Here, we introduce generalised Maxwell relations that relate every thermodynamic quantity to a single local correlation function. We illustrate their utility by deducing the thermodynamic properties of several iconic quantum many-body models from pair correlation functions using the generalised Maxwell relations. We show that this universal approach is readily accessible in quantum simulators and suggest applications to condensed matter systems where thermodynamic measurements are challenging, such as atomically thin materials.

Condensed matter physics is entering an era of unprecedented control over the design and synthesis of quantum materials. Engineered materials such as metal-organic frameworks [1], twistrionics devices [2, 3] and atomically thin 2D materials [4–6] have emergent properties that may enable breakthrough applications from tackling climate change to the quantum technology revolution. However, emerging properties are difficult to predict [7], making it challenging to exploit this structural control to achieve new functionalities.

One possible approach to designing new quantum materials is to harness the rapidly increasing potential of quantum simulators—precursors to general purpose quantum computers that allow the accurate simulation of a single model [8]. The most advanced quantum simulators include ultracold atoms in optical lattice potentials [9–11] (Fig. 1a) or tweezer arrays [12, 13], quantum dot arrays [14], superconducting circuits [15, 16] and ion traps [17–20] (Fig. 1b). All offer precise control of the underlying Hamiltonian, rarely possible in traditional condensed matter systems. Therefore, they are ideal test beds for theory and provide platforms for understanding and engineering emergent physics. Superfluidity, topological phases, and metal-insulator transitions have been demonstrated in these devices. However, in quantum simulators, it is much easier to measure correlation functions [9–20] than the thermodynamic variables that have provided invaluable insights in traditional condensed matter systems, from uncovering new states of matter to understanding universality in phase transitions. Furthermore, as thermodynamic measurements remain a mainstay of materials characterisation and condensed matter physics, this limits our ability to compare quantum simulations to experiments on the materials being modelled.

Here, we propose a new *universal* method of extracting *any* thermodynamic quantity from measurements of a single correlation function. To do this we generalise Maxwell relations—which allow one thermodynamic quantity to be determined from measurements of another [21]—to include cor-

relation functions; Fig. 1. This contrasts with previous attempts to extract thermodynamics from correlation functions [22, 23] or Tan’s contact [24, 25] that are formulated for specific models or require (experimentally challenging) measurements of high-energy tails of momentum distributions. Our method requires only measurements of local pair correlation, making it broadly applicable to a wide range of systems. Thus, this work opens the door to widespread measurements of the thermodynamic properties in quantum simulators.

We validate the generalised Maxwell relations, by using them to calculate the properties of well-studied problems including Bose and Fermi gases, Mott transitions, and magnetic quantum phase transitions. Extracting thermodynamic properties from experimentally measured correlation functions would follow the same logic. Thus, this demonstrates the utility of our approach as a tool for both theory and experiment.

We also use the generalised Maxwell relations to calculate an analytical expression for the entropy of a strongly interaction Fermi gas, demonstrating the ease with which new theory can be developed using this method.

Finally, we find that the integrated correlation function, introduced below and key to our approach, is a thermodynamic variable. We demonstrate that this can therefore be used to probe phase transitions in materials where it is difficult or impossible to measure conventional thermodynamic properties, such as 2D materials.

Model systems and correlation functions

The derivation of the generalised Maxwell relations is, almost embarrassingly, simple but requires a few definitions, which we give in this section.

We begin by considering a quantum many-body interacting system with pairwise interactions, characterised by the Hamiltonian

$$\hat{H} = \hat{H}_0 + c\hat{G}_2. \quad (1)$$

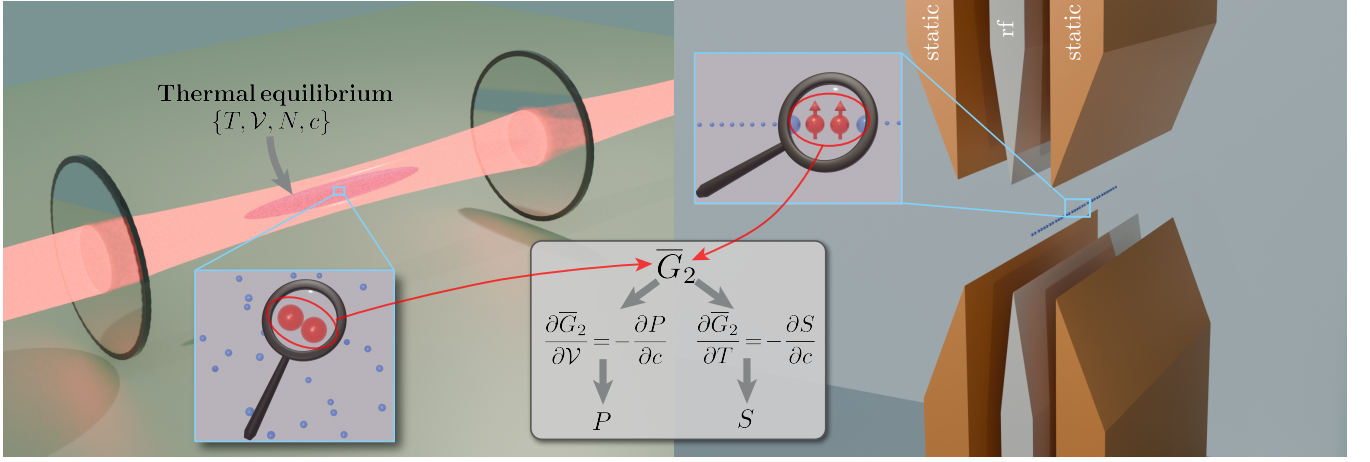


FIG. 1. An illustration of the key idea behind this work: a quantum gas microscope (left) or an ion trap (right) measures the two-atom or two-spin integrated correlation \overline{G}_2 as a function of the interaction strength c and other thermodynamic parameters such as temperature (T), system size (\mathcal{V}), number of particles (N), etc.; the Maxwell relations derived here allow for an arbitrary thermodynamic quantity—such as pressure P , entropy S , chemical potential, heat capacity, magnetization, etc.—to be deduced from the measured \overline{G}_2 .

Here, \hat{H}_0 is the non-interacting Hamiltonian, c parametrises the strength of two-body interactions, and \hat{G}_2 is a two-body operator, which we will refer to as an integrated pair correlation for reasons that will become clear shortly.

For many paradigmatic many-body models the operator \hat{G}_2 can be expressed as an integral or sum over creation, annihilation, or spin operators, such as:

$$\hat{G}_2 = \begin{cases} \iint d\mathbf{r}d\mathbf{r}' \hat{\Psi}^\dagger(\mathbf{r}) \hat{\Psi}^\dagger(\mathbf{r}') f(\mathbf{r}, \mathbf{r}') \hat{\Psi}(\mathbf{r}') \hat{\Psi}(\mathbf{r}). & (2a) \\ \sum_j \hat{c}_{j,\uparrow}^\dagger \hat{c}_{j,\uparrow} \hat{c}_{j,\downarrow}^\dagger \hat{c}_{j,\downarrow}, & (2b) \\ \sum_j \hat{S}_j^z \hat{S}_{j+1}^z. & (2c) \end{cases}$$

Equation (2a) describes the interactions in a gas of identical bosons, annihilated (created) at position \mathbf{r} by the field operator $\hat{\Psi}^\dagger(\mathbf{r})$, with $f(\mathbf{r}, \mathbf{r}')$ describing the spatial dependence of the interaction. Equation (2b) is the Fermi-Hubbard interaction between fermions annihilated (created) at site j with spin σ by the operator $\hat{c}_{j,\sigma}^\dagger$. Equation (2c) is the Ising interaction between the z -components, \hat{S}_j^z , of adjacent spins on a lattice.

The expectation value

$$\overline{G}_2 \equiv \langle \hat{G}_2 \rangle, \quad (3)$$

is proportional to an integral or a sum over local correlation functions. For example, the Lieb-Liniger model [26] (see Methods) of a 1D Bose gas assumes contact interactions, $f(x, x') = \delta(x - x')$. For a uniform system of length \mathcal{V} the integrated correlation is proportional to the local two-particle correlation function: $\overline{G}_2 = \mathcal{V}G^{(2)} = \mathcal{V}\langle \hat{\Psi}^\dagger(x) \hat{\Psi}^\dagger(x) \hat{\Psi}(x) \hat{\Psi}(x) \rangle$.

Maxwell relations for pair correlation functions

Standard Maxwell relations follow [21] from the commutativity of mixed second derivatives of the Helmholtz free energy, F . Here we generalise this derivation by taking derivatives with respect to the interaction strength c and a standard thermodynamic parameter, X :

$$\left[\frac{\partial}{\partial c} \left(\frac{\partial F}{\partial X} \right)_{c,\dots} \right]_{X,\dots} = \left[\frac{\partial}{\partial X} \left(\frac{\partial F}{\partial c} \right)_{X,\dots} \right]_{c,\dots}, \quad (4)$$

where the ellipsis represents all the other external parameters held fixed. In the canonical formulation of statistical mechanics, which we adopt here (see Supplementary Information for formulation in other ensembles), X can be, for example, the temperature, T , the total number of particles, N , or the system size, \mathcal{V} , (i.e., volume in 3D; area in 2D; or length in 1D). $Y = (\partial F / \partial X)_{c,\dots}$, is then a thermodynamic quantity, such as pressure, entropy, chemical potential, depending on the choice of X . Similarly, $(\partial F / \partial c)_{X,\dots} = \overline{G}_2$ (see Methods and Supplementary Information). This yields the generalised Maxwell relation

$$\left(\frac{\partial Y}{\partial c} \right)_{X,\dots} = \left(\frac{\partial \overline{G}_2}{\partial X} \right)_{c,\dots}, \quad (5)$$

Integrating the generalised Maxwell relation, equation (5), from some c_0 to c , where $Y(c_0)$ is known, allows one to evaluate $Y(c)$ from the measured or calculated derivative of the integrated correlation function:

$$Y(c) = Y(c_0) + \int_{c_0}^c \left(\frac{\partial \overline{G}_2(c')}{\partial X} \right)_{c',\dots} dc'. \quad (6)$$

The generalised Maxwell relations can straightforwardly be extended to treat second derivatives of the free energy. One

finds (see Methods) that if $Y = (\partial^2 F / \partial X \partial X')$, then

$$\left(\frac{\partial Y}{\partial c}\right)_{X, X', \dots} = \left(\frac{\partial^2 \overline{G}_2}{\partial X \partial X'}\right)_{c, \dots}. \quad (7)$$

On integrating, one finds that

$$Y(c) = Y(c_0) + \int_{c_0}^c \left(\frac{\partial^2 \overline{G}_2(c')}{\partial X \partial X'}\right)_{c', \dots} dc'. \quad (8)$$

Second derivatives of the free energy, such as heat capacity, magnetic susceptibility, or isothermal compressibility play a crucial role in thermodynamics, for example, in probing continuous phase transitions (also known as second order phase transitions).

The differential (equations (5) and (7)) and integral (equations (6) and (8)) forms of the generalised Maxwell relations are the key results of this work. They imply that any thermodynamic quantity, Y , can be determined from the measurements of the correlation function \overline{G}_2 . To illustrate the utility of generalised Maxwell relations we discuss several possible choices for the thermodynamic quantities X and Y below; the differential forms of the respective Maxwell relations are summarised in Table I (for the integral forms, see Supplementary Information).

TABLE I. Maxwell relations between various thermodynamic quantities and the pair correlation \overline{G}_2 .

Thermodynamic quantity	Maxwell relation with \overline{G}_2	Eq.
Pressure, P	$\left(\frac{\partial P}{\partial c}\right)_{\nu, T, N} = -\left(\frac{\partial \overline{G}_2}{\partial \nu}\right)_{c, T, N}$	(9)
Entropy, S	$\left(\frac{\partial S}{\partial c}\right)_{T, \nu, N} = -\left(\frac{\partial \overline{G}_2}{\partial T}\right)_{c, \nu, N}$	(10)
Chemical potential, μ	$\left(\frac{\partial \mu}{\partial c}\right)_{T, \nu, N} = \left(\frac{\partial \overline{G}_2}{\partial N}\right)_{c, T, \nu}$	(11)
Magnetization, m	$\left(\frac{\partial m}{\partial c}\right)_{\mathbf{h}, T, \nu, N} = -\left(\nabla_{\mathbf{h}} \overline{G}_2\right)_{c, T, \nu, N}$	(12)
Heat capacity, C_ν	$\left(\frac{\partial C_\nu}{\partial c}\right)_{T, \nu, N} = -T \left(\frac{\partial^2 \overline{G}_2}{\partial T^2}\right)_{c, \nu, N}$	(13)
Isothermal compressibility, κ_T	$\left(\frac{\partial \kappa_T^{-1}}{\partial c}\right)_{T, \nu, N} = \nu \left(\frac{\partial^2 \overline{G}_2}{\partial \nu^2}\right)_{T, N, c}$	(14)

Bose and Fermi gases

Pressure ($Y \equiv -P$, $X \equiv \nu$). For pressure, $P = -(\partial F / \partial \nu)_{T, N, c}$, the differential form of the generalised Maxwell relation (5) takes the form of Eq. (9), Table I (for the integral form, see Supplementary Information).

The Lieb-Liniger model provides a simple context for exploring these relations. In the weakly interacting regime ($c \ll \hbar^2 n / m$, where m is the mass of the bosons and $n = N / \nu$ is the particle number density) and at zero temperature, one can use the mean-field approximation. In this regime, density-density fluctuations are uncorrelated, and therefore

$\overline{G}^{(2)} = N^2 / \nu$. The standard derivation of the non-trivial result $P(c) = -(\partial U_0 / \partial \nu)_{T, N, c} = cn^2$ [27, 28], at zero temperature, requires the calculation of the ground state energy, U_0 . However, this result is much more easily obtained from the generalised Maxwell relation. Trivially, $(\partial \overline{G}_2 / \partial \nu)_{c, T, N} = -N^2 / \nu^2 = -n^2$. On choosing $c_0 = 0$ and noting that $P(0) = 0$, Eqs. (6) and (9) immediately yield $P(c) = cn^2$. (This derivation can be easily extended to 2D and 3D systems.) Thus, it is much easier to calculate the pressure from the correlation function than via standard thermodynamic approaches for this system.

The generalised Maxwell equation approach also allows more straightforward calculations of thermodynamic properties in highly non-trivial regimes, for example the strongly interacting 1D Bose gas ($c > \hbar^2 n / m$). In this limit thermodynamic properties can be calculated exactly using the thermodynamic Bethe ansatz (TBA) [31]. We benchmark our Maxwell relations, Eqs. (6) and (9), against the exact results by numerically evaluating $\overline{G}_2(c)$ via the density matrix renormalisation group (DMRG; see Methods and Supplementary Information) [32, 33]. The two methods are in excellent agreement for the pressure (Fig. 2a) and the isothermal compressibility (Supplementary Information).

The equivalent model for spin-1/2 fermions in 1D is known as the Yang-Gaudin model [34, 35] (see Methods). Although this model is also exactly solvable using the TBA, approximate analytical results for thermodynamic quantities are scarce outside of the low-temperature Luttinger liquid regime [36]. In the Supplementary Information we show that in the high-temperature limit,

$$S \simeq S_{\text{IFG}} - \frac{N(1 - \mathcal{P}^2)}{16\hbar} \sqrt{\frac{\pi m}{2k_B T^3}} n c^2. \quad (15)$$

where S_{IFG} is the entropy of the ideal Fermi gas and \mathcal{P} is the polarisation. The simplicity of the derivation of this result highlights the power of the generalised Maxwell equations for making progress with otherwise intractable problems.

The Mott transition

Mott insulators are of fundamental interest because of their role in high-temperature and unconventional superconductors [37], and because of potential applications, including ultrafast transistors, volatile and non-volatile memories, and artificial neurons for neuromorphic computing [5, 38]. As such, Mott insulators have been a target for many quantum simulators [10, 11].

Chemical potential ($Y \equiv \mu$, $X \equiv N$). The generalised Maxwell equation for the chemical potential, μ , takes the form of Eq. (11) in Table I. As a proof-of-principle study of the Mott transition, we calculated the zero temperature, local correlation functions, and the ground state energies of the 1D Fermi- and Bose-Hubbard models using DMRG (see Methods). The chemical potentials of both models calculated from the generalised Maxwell relations are in excellent agreement with direct calculations using $\mu = (\partial F / \partial N)_{T, \nu, c}$, Figs. 2b,

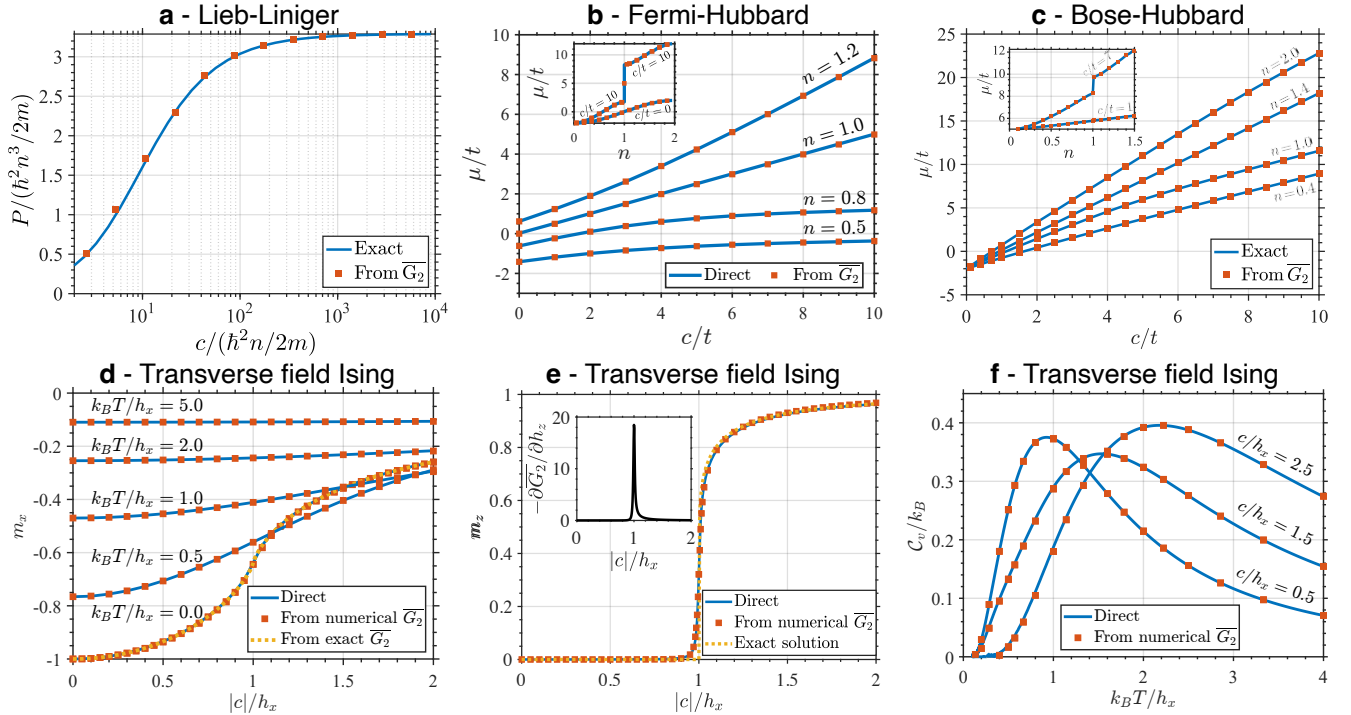


FIG. 2. Comparison of thermodynamic quantities calculated from: (i) the integrated correlation function, \overline{G}_2 , using the Maxwell relations derived here and numerically calculated correlation functions (red squares), and (ii) traditional methods of statistical mechanics either directly from our numerics (blue curves) or from exact results (yellow dashed curves). In all cases the agreement between the two methods is excellent. **a**, Pressure, P , of the strongly interacting Lieb-Liniger gas at $T = 0$ K. Chemical potentials, μ , of the 1D, **b**, Fermi- and, **c**, Bose-Hubbard models, where c is the on-site interaction and t is the hopping integral. The insets show the chemical potential as a function of filling, n . The discontinuities in the chemical potentials when the number of particles equals the number of sites ($n = 1$) for large c/t , indicate (Mott) metal-insulator transitions [29, 30]. **d**, Transverse magnetisation, m_x (see Supplementary Information for derivation of the exact result), **e**, longitudinal magnetisation, m_z , and **f**, heat capacity, C_V , of the transverse field Ising model for field strength h_x . This demonstrates that, although C_V is the second derivative of the free energy, it can also be calculated essentially exactly from \overline{G}_2 . Inset to **e**, the derivative of the pair correlation function \overline{G}_2 diverges at the critical point $|c| = h_x$, providing a signature of the continuous phase transition. This highlights that \overline{G}_2 is a thermodynamic variable.

c. For sufficiently strong interactions, a Mott gap opens at $n = 1$ in both models (insets to Figs. 2b, c), indicated by a discontinuous increase in the chemical potential [29, 30, 39]. Importantly, the size of the Mott gap (i.e., the magnitude of the discontinuous increase in μ) is also in excellent agreement for both methods, indicating that thermodynamics extracted from correlation functions reliably describe Mott physics in the strongly correlated regime.

Magnetic insulators: the transverse field Ising model

Capturing the physics near a phase transition requires extremely high accuracy experiments or calculations. Therefore, it is important to benchmark the accuracy of the thermodynamics extracted from correlation functions close to phase transitions as this provides a stringent test of the generalised Maxwell relations. Therefore, we consider the transverse field Ising model, which is the simplest model that shows a quantum phase transition (i.e., a continuous phase transition at zero temperature) [40], and has been a key target for quantum simulators [8, 15–20].

Magnetization ($Y = -m$, $X = \mathbf{h}$). In an external magnetic field, $\mathbf{h} = \hat{\mathbf{i}}h_x + \hat{\mathbf{j}}h_y + \hat{\mathbf{k}}h_z$, the magnetization is $\mathbf{m} = \hat{\mathbf{i}}m_x + \hat{\mathbf{j}}m_y + \hat{\mathbf{k}}m_z = -\mathcal{V}^{-1}(\nabla_{\mathbf{h}}F)_{T,\mathcal{V},N,c}$, where $\nabla_{\mathbf{h}} = \hat{\mathbf{i}}(\partial/\partial h_x) + \hat{\mathbf{j}}(\partial/\partial h_y) + \hat{\mathbf{k}}(\partial/\partial h_z)$. The relevant generalised Maxwell relation is given in Eq. (12).

We calculated the magnetization of the ferromagnetic ($c < 0$) transverse field Ising model (see Methods) by: (i) applying Eqs. (6) and (12) to the \overline{G}_2 computed with thermal DMRG, where we take $c_0 = 0$, the limit of non-interacting spins; (ii) applying Eqs. (6) and (12) to the \overline{G}_2 calculated exactly at $T = 0$ (Supplementary Information); and (iii) directly evaluating $m_x = (1/\mathcal{V}) \sum_{j=1}^{\mathcal{V}} \langle \hat{S}_j^x \rangle$ using DMRG. All three methods are in excellent agreement, Fig. 2d.

The transverse field Ising model at $T = 0$ has a quantum critical point at $h_x = |c|$ [40]. The system is ferromagnetically ordered ($m_z \neq 0$) for $|c| > h_x$, whereas it is quantum disordered for $|c| < h_x$ (hence $m_z = 0$). This provides an ideal test case. The magnetization calculated via \overline{G}_2 agrees well with the exact solution [41, 42], Fig. 2e. However, there is some disagreement very close to the quantum critical

point. The agreement between the magnetization calculated from \overline{G}_2 and directly from DMRG shows that the disagreement with the exact result is due to the limitations of DMRG near the critical point rather than any issue with the generalised Maxwell relation. Thus, we conclude that the generalised Maxwell relation holds in the most stringent of conditions, close to a critical point.

Interestingly, close to the quantum critical point the $\partial\overline{G}_2/\partial h_z$ displays a ‘lambda’ anomaly, Fig. 2e (inset), providing a clear signature of the continuous phase transition and allowing the measurement of critical exponents (see Supplementary Information). This is because the integrated correlation function is a thermodynamic function and therefore provides direct thermodynamic information. As $\partial\overline{G}_2/\partial h_z = (\partial^2 F/\partial c \partial h_z)_{T,\nu,N}$ is a second derivative of the free energy, it should be expected to display a lambda anomaly at the critical point—exactly as we find in our calculations. Thus, measurements of integrated correlation functions provide a new method to characterise phase transitions in quantum many-body systems.

This provides a useful approach for probing the physics of engineered quantum systems, such as 2D materials. Conventional thermodynamics is challenging in such systems—for example the heat capacity is typically dominated by the substrate. Relevant correlation functions might be measured via local electron tunnelling spectroscopic probes [43–45].

Heat capacity ($Y = -C_V/T$, $X = X' = T$). Like many of the most frequently measured thermodynamic quantities, the heat capacity is a second derivative of the free energy. In this case, the generalised Maxwell relation (7) between the (constant volume) heat capacity, $C_V = -T (\partial^2 F/\partial T^2)_{N,\nu,c}$, and the integrated correlation function, \overline{G}_2 , is given by Eq. (13), Table I.

To test this Maxwell relation we computed C_V for the transverse field Ising model from: (i) the calculated \overline{G}_2 via Eqs. (6) and (13) with $c_0 = 0$; and (ii) the variance of the energy [21]. Both calculations are in excellent agreement, Fig. 2f. Similar agreement with standard thermodynamics is found for the isothermal compressibility of the Bose gas (Supplementary Information). Both results confirm the accuracy of the generalised Maxwell relation approach for second derivatives of the free energy.

Conclusions

The generalised Maxwell relations, derived above, provide a powerful, universal approach to measuring the thermodynamics of quantum simulators and other systems where it is significantly easier to measure correlation functions than to perform traditional thermodynamic measurements. These relations bridge the gap between microscopic measurements and macroscopic properties by linking observables such as pressure, entropy, and heat capacity to derivatives of correlation functions, thereby extending the traditional paradigm of macroscopic thermodynamics.

While, in this paper, we have limited our discussion to pair-

wise interactions and pair correlation functions, Maxwell relations can be straightforwardly generalised to higher-body interactions with the pair correlation function replaced by the appropriate higher order correlation function.

Many quantum simulators allow the interaction strength, c , to be continuously varied, enabling the integrals required to evaluate thermodynamic properties (equations (6) and (8)) to be evaluated from experimental data. In conventional materials this is typically not possible. Nevertheless, as shown above, the integrated correlation function, \overline{G}_2 , is itself a thermodynamic variable. Thus, direct measurement of local correlation functions will enable thermodynamic measurements in systems, such as 1D and 2D materials, where traditional thermodynamic measurements are not possible, for example, due to such measurements being dominated by a substrate.

Conversely, in many materials thermodynamic measurements are straightforward while the most interesting correlation functions cannot be measured. For example, magnetic systems that cannot be grown in large enough single crystals to enable inelastic neutron scattering. The generalised Maxwell relations could provide significant insights into correlations in such materials by inverting our approach, i.e., by extracting integrated correlation functions from traditional measurements of thermodynamic quantities.

Finally, we note that thermometry is difficult in some quantum simulators, e.g., quantum gas microscopes. The generalised Maxwell relations may offer a solution to this by determining the temperature from measurements of the integrated correlation functions.

* powell@physics.uq.edu.au

† karen.kheruntsyan@uq.edu.au

- [1] M. J. Kalmutzki, N. Hanikel, and O. M. Yaghi, Secondary building units as the turning point in the development of the reticular chemistry of MOFs, *Sci. Adv.* **4**, eaat9180 (2018).
- [2] Y. Cao, V. Fatemi, S. Fang, K. Watanabe, T. Taniguchi, E. Kaxiras, and P. Jarillo-Herrero, Unconventional superconductivity in magic-angle graphene superlattices, *Nature* **556**, 43 (2018).
- [3] Y. Xia, Z. Han, K. Watanabe, T. Taniguchi, J. Shan, and K. F. Mak, Superconductivity in twisted bilayer WSe₂, *Nature* **637**, 833 (2025).
- [4] M. J. Kalmutzki, N. Hanikel, and O. M. Yaghi, Secondary building units as the turning point in the development of the reticular chemistry of MOFs, *Sci. Adv.* **4**, eaat9180 (2018).
- [5] B. Lowe, B. Field, J. Hellerstedt, J. Ceddia, H. L. Nourse, B. J. Powell, N. V. Medhekar, and A. Schiffrin, Local gate control of Mott metal-insulator transition in a 2D metal-organic framework, *Nat. Comm.* **15**, 3559 (2024).
- [6] T. Takenaka, K. Ishihara, M. Roppongi, Y. Miao, Y. Mizukami, T. Makita, J. Tsurumi, S. Watanabe, J. Takeya, M. Yamashita, K. Torizuka, Y. Uwatoko, T. Sasaki, X. Huang, W. Xu, D. Zhu, N. Su, J.-G. Cheng, T. Shibauchi, and K. Hashimoto, Strongly correlated superconductivity in a copper-based metal-organic framework with a perfect kagome lattice, *Sci. Adv.* **7**, eabf3996 (2021).
- [7] B. J. Powell, Emergent particles and gauge fields in quantum

- matter, *Contemp. Phys.* **61**, 96 (2020).
- [8] B. Fauseweh, Quantum many-body simulations on digital quantum computers: State-of-the-art and future challenges, *Nat. Comm.* **15**, 2123 (2024).
- [9] C. Gross and I. Bloch, Quantum simulations with ultracold atoms in optical lattices, *Science* **357**, 995 (2017).
- [10] M. F. Parsons, A. Mazurenko, C. S. Chiu, G. Ji, D. Greif, and M. Greiner, Site-resolved measurement of the spin-correlation function in the Fermi-Hubbard model, *Science* **353**, 1253 (2016).
- [11] D. Bourgund, T. Chalopin, P. Bojović, H. Schlömer, S. Wang, T. Franz, S. Hirthe, A. Bohrdt, F. Grusdt, I. Bloch, and T. A. Hilker, Formation of individual stripes in a mixed-dimensional cold-atom Fermi-Hubbard system, *Nature* **637**, 57 (2025).
- [12] S. Ebadi, T. T. Wang, H. Levine, A. Keesling, G. Semeghini, A. Omran, D. Bluvstein, R. Samajdar, H. Pichler, W. W. Ho, S. Choi, S. Sachdev, M. Greiner, V. Vuletić, and M. D. Lukin, Quantum phases of matter on a 256-atom programmable quantum simulator, *Nature* **595**, 227 (2021).
- [13] G. Semeghini, H. Levine, A. Keesling, S. Ebadi, T. T. Wang, D. Bluvstein, R. Verresen, H. Pichler, M. Kalinowski, R. Samajdar, A. Omran, S. Sachdev, A. Vishwanath, M. Greiner, V. Vuletić, and M. D. Lukin, Probing topological spin liquids on a programmable quantum simulator, *Science* **374**, 1242 (2021).
- [14] T. Hensgens, T. Fujita, L. Janssen, X. Li, C. J. Van Diepen, C. Reichl, W. Wegscheider, S. Das Sarma, and L. M. K. Vander-sypen, Quantum simulation of a Fermi-Hubbard model using a semiconductor quantum dot array, *Nature* **548**, 70 (2017).
- [15] M. Kjaergaard, M. E. Schwartz, J. Braumüller, P. Krantz, J. I.-J. Wang, S. Gustavsson, and W. D. Oliver, Superconducting qubits: Current state of play, *Annu. Rev. Condens. Matter Phys.* **11**, 369 (2020).
- [16] Y. Salathé, M. Mondal, M. Oppliger, J. Heinsoo, P. Kurpiers, A. Potočnik, A. Mezzacapo, U. Las Heras, L. Lamata, E. Solano, S. Filipp, and A. Wallraff, Digital quantum simulation of spin models with circuit quantum electrodynamics, *Phys. Rev. X* **5**, 021027 (2015).
- [17] C. Monroe, W. C. Campbell, L.-M. Duan, Z.-X. Gong, A. V. Gorshkov, P. W. Hess, R. Islam, K. Kim, N. M. Linke, G. Pagano, P. Richerme, C. Senko, and N. Y. Yao, Programmable quantum simulations of spin systems with trapped ions, *Rev. Mod. Phys.* **93**, 025001 (2021).
- [18] S.-A. Guo, Y.-K. Wu, J. Ye, L. Zhang, W.-Q. Lian, R. Yao, Y. Wang, R.-Y. Yan, Y.-J. Yi, Y.-L. Xu, B.-W. Li, Y.-H. Hou, Y.-Z. Xu, W.-X. Guo, C. Zhang, B.-X. Qi, Z.-C. Zhou, L. He, and L.-M. Duan, A site-resolved two-dimensional quantum simulator with hundreds of trapped ions, *Nature* **630**, 613 (2024).
- [19] K. Kim, M.-S. Chang, S. Korenblit, R. Islam, E. E. Edwards, J. K. Freericks, G.-D. Lin, L.-M. Duan, and C. Monroe, Quantum simulation of frustrated Ising spins with trapped ions, *Nature* **465**, 590 (2010).
- [20] B. P. Lanyon, C. Hempel, D. Nigg, M. Müller, R. Geritsma, F. Zähringer, P. Schindler, J. T. Barreiro, M. Rambach, G. Kirchmair, M. Hennrich, P. Zoller, R. Blatt, and C. F. Roos, Universal digital quantum simulation with trapped ions, *Science* **334**, 57 (2011).
- [21] H. B. Callen, *Thermodynamics and an Introduction to Thermostatistics* (John Wiley & Sons, New York, 1985).
- [22] F. Werner, O. Parcollet, A. Georges, and S. R. Hassan, Interaction-induced adiabatic cooling and antiferromagnetism of cold fermions in optical lattices, *Phys. Rev. Lett.* **95**, 056401 (2005).
- [23] R. S. Watson, C. Coleman, and K. V. Kheruntsyan, Maxwell relation between entropy and atom-atom pair correlation, *Phys. Rev. Lett.* **133**, 100403 (2024).
- [24] Y.-Y. Chen, Y.-Z. Jiang, X.-W. Guan, and Q. Zhou, Critical behaviours of contact near phase transitions, *Nat. Comm.* **5**, 5140 (2014).
- [25] W. E. Liu, Z.-Y. Shi, M. M. Parish, and J. Levinsen, Theory of radio-frequency spectroscopy of impurities in quantum gases, *Phys. Rev. A* **102**, 023304 (2020).
- [26] E. H. Lieb and W. Liniger, Exact analysis of an interacting Bose gas. I. The general solution and the ground state, *Phys. Rev.* **130**, 1605 (1963).
- [27] C. Pethick and H. Smith, *Bose-Einstein condensation in dilute gases*, 2nd ed. (Cambridge University Press, Cambridge, UK ; New York, 2008).
- [28] M. L. Kerr, G. D. Rosi, and K. V. Kheruntsyan, Analytic thermodynamic properties of the Lieb-Liniger gas, *SciPost Phys. Core* **7**, 047 (2024).
- [29] E. H. Lieb and F. Y. Wu, Absence of Mott Transition in an Exact Solution of the Short-Range, One-Band Model in One Dimension, *Phys. Rev. Lett.* **20**, 1445 (1968).
- [30] E. H. Lieb and F. Wu, The one-dimensional Hubbard model: a reminiscence, *Physica A: Stat. Mech. Appl.* **321**, 1 (2003).
- [31] C.-N. Yang and C. P. Yang, Thermodynamics of a one-dimensional system of bosons with repulsive delta-function interaction, *J. Math. Phys.* **10**, 1115 (1969).
- [32] S. R. White, Density matrix formulation for quantum renormalization groups, *Phys. Rev. Lett.* **69**, 2863 (1992).
- [33] U. Schollwöck, The density-matrix renormalization group in the age of matrix product states, *Ann. Phys. (N. Y.)* **326**, 96 (2011).
- [34] C. N. Yang, Some Exact Results for the Many-Body Problem in one Dimension with Repulsive Delta-Function Interaction, *Phys. Rev. Lett.* **19**, 1312 (1967).
- [35] M. Gaudin, Un système a une dimension de fermions en interaction, *Phys. Lett. A* **24**, 55 (1967).
- [36] E. Zhao, X.-W. Guan, W. V. Liu, M. T. Batchelor, and M. Oshikawa, Analytic thermodynamics and thermometry of gaudin-yang fermi gases, *Phys. Rev. Lett.* **103**, 140404 (2009).
- [37] P. A. Lee, N. Nagaosa, and X.-G. Wen, Doping a Mott insulator: Physics of high-temperature superconductivity, *Rev. Mod. Phys.* **78**, 17 (2006).
- [38] A. Milloch, M. Fabrizio, and C. Giannetti, Mott materials: unsuccessful metals with a bright future, *npj Spintronics* **2**, 49 (2024).
- [39] S.-D. Ouyang, J. Liu, S.-H. Xiang, and K.-H. Song, Ground State Property of a One-Dimensional Bose-Hubbard Model Using Time-Evolving Body Decimation, *Chin. Phys. Lett.* **30**, 086701 (2013).
- [40] S. Sachdev, *Quantum Phase Transitions*, 2nd ed. (Cambridge University Press, Cambridge, UK ; New York, 2011).
- [41] B. M. McCoy, Spin Correlation Functions of the $X - Y$ Model, *Phys. Rev.* **173**, 531 (1968).
- [42] P. Pfeuty, The one-dimensional Ising model with a transverse field, *Ann. Phys. (N. Y.)* **57**, 79 (1970).
- [43] M. Leeuwenhoek, S. Gröblacher, M. P. Allan, and Y. M. Blanter, Modeling Green's function measurements with two-tip scanning tunneling microscopy, *Phys. Rev. B* **102**, 115416 (2020).
- [44] Q. Niu, M. C. Chang, and C. K. Shih, Double-tip scanning tunneling microscope for surface analysis, *Phys. Rev. B* **51**, 5502 (1995).
- [45] J. M. Byers and M. E. Flatté, Probing spatial correlations with nanoscale two-contact tunneling, *Phys. Rev. Lett.* **74**, 306 (1995).
- [46] H. Hellmann, Zur Rolle der kinetischen Elektronenenergie für

die zwischenatomaren Kräfte, *Z. Phys.* **85**, 180 (1933).

- [47] R. P. Feynman, Forces in molecules, *Phys. Rev.* **56**, 340 (1939).
 [48] K. V. Kheruntsyan, D. M. Gangardt, P. D. Drummond, and G. V. Shlyapnikov, Pair correlations in a finite-temperature 1D Bose gas, *Phys. Rev. Lett.* **91**, 040403 (2003).
 [49] S. A. Simmons, F. A. Bayocoboc, J. C. Pillay, D. Colas, I. P. McCulloch, and K. V. Kheruntsyan, What is a quantum shock wave?, *Phys. Rev. Lett.* **125**, 180401 (2020).
 [50] X.-W. Guan, M. T. Batchelor, and C. Lee, Fermi gases in one dimension: From bethe ansatz to experiments, *Rev. Mod. Phys.* **85**, 1633 (2013).
 [51] A. E. Feiguin and S. R. White, Finite-temperature density matrix renormalization using an enlarged Hilbert space, *Phys. Rev. B* **72**, 220401 (2005).
 [52] A. Savitzky and M. Goly, Smoothing and Differentiation of Data by Simplified Least Squares Procedures, *Anal. Chem.* **36**, 1627 (1964).
 [53] R. A. Alberty, Use of Legendre transforms in chemical thermodynamics (IUPAP Technical Report), *J. Chem. Thermodyn.* **34**, 1787 (2002).
 [54] O. I. Pâtu and A. Klümper, Thermodynamics, contact, and density profiles of the repulsive Gaudin-Yang model, *Phys. Rev. A* **93**, 033616 (2016).
 [55] S. Tan, Large momentum part of a strongly correlated Fermi gas, *Ann. Phys. (N. Y.)* **323**, 2971 (2008).
 [56] S. Tan, Generalized virial theorem and pressure relation for a strongly correlated Fermi gas, *Ann. Phys. (N. Y.)* **323**, 2987 (2008).
 [57] M. Barth and W. Zwerger, Tan relations in one dimension, *Ann. Phys. (N. Y.)* **326**, 2544 (2011).
 [58] W.-B. He, Y.-Y. Chen, S. Zhang, and X.-W. Guan, Universal properties of Fermi gases in one dimension, *Phys. Rev. A* **94**, 031604 (2016).

Methods

Maxwell relations

The generalised Maxwell relations involving correlation functions are derived here in the canonical formalism of statistical mechanics. The Helmholtz free energy, F , is given by

$$F = -k_B T \ln \left(\text{Tr} e^{-\hat{H}/k_B T} \right). \quad (16)$$

Applying the Hellmann-Feynman theorem [46–48] to the general Hamiltonian for pairwise interactions, equation (1), one finds that

$$\frac{\partial F}{\partial c} = \frac{1}{Z} \text{Tr} \left(e^{-\hat{H}/k_B T} \frac{\partial \hat{H}}{\partial c} \right) = \overline{G_2}, \quad (17)$$

where $Z = \text{Tr} \exp(-\hat{H}/k_B T)$ is the partition function. Whence, the generic form of Maxwell relations, equation (5), follows from the commutativity of mixed second derivatives, equation (4).

In the Supplementary Information we show how the same Maxwell relations can be derived (i) without resorting to the Hellmann-Feynman theorem but instead starting from the observation that c and $\overline{G_2}$ are conjugate thermodynamic parameters; and (ii) in other thermodynamic ensembles.

Lieb-Liniger model

The Lieb-Liniger model of a uniform gas of N bosons interacting in 1D via pairwise contact (δ -function) interaction is specified by equation (1), with

$$\hat{H}_0 = -\frac{\hbar^2}{2m} \int_0^\nu dx \hat{\Psi}^\dagger(x) \frac{\partial^2 \hat{\Psi}(x)}{\partial x^2}, \quad (18)$$

$$\hat{G}_2 = \int_0^\nu dx \hat{\Psi}^\dagger(x) \hat{\Psi}^\dagger(x) \hat{\Psi}(x) \hat{\Psi}(x). \quad (19)$$

In the strongly interacting limit the integrated correlation function $\overline{G_2}(c)$ is calculated at $T = 0$ using DMRG following [49]. The integral form of the generalised Maxwell relation for pressure, Eq. (9), then allows us to compute $P(c)$ (shown in Fig. 2a) after setting $c_0 \rightarrow \infty$, which corresponds to the strongly interacting Tonks-Girardeau limit of the 1D Bose gas, for which the pressure is identical to that of the 1D non-interacting spinless Fermi gas (see, e.g., [28]).

Yang-Gaudin model

The Yang-Gaudin model [34, 35, 50] is similar to the Lieb-Liniger model, except that it describes a system of interacting spin-1/2 fermions in 1D. The corresponding Hamiltonian can be written as a sum of two terms:

$$\hat{H}_0 = -\sum_{\sigma=\uparrow,\downarrow} \frac{\hbar^2}{2m} \int_0^\nu dx \hat{\Psi}_\sigma^\dagger(x) \frac{\partial^2 \hat{\Psi}_\sigma(x)}{\partial x^2}, \quad (20)$$

$$\hat{G}_2 = \int_0^\nu dx \hat{\Psi}_\uparrow^\dagger(x) \hat{\Psi}_\downarrow^\dagger(x) \hat{\Psi}_\downarrow(x) \hat{\Psi}_\uparrow(x), \quad (21)$$

where the field operators $\hat{\Psi}_\sigma^{(\dagger)}(x)$ annihilate (create) a fermion with spin $\sigma = \uparrow, \downarrow$ at position x .

Fermi- and Bose-Hubbard models

The Fermi-Hubbard model is specified by

$$\hat{H}_0 = -t \sum_{j=1}^\nu \sum_{\sigma=\uparrow,\downarrow} \left(\hat{c}_{j,\sigma}^\dagger \hat{c}_{j+1,\sigma} + \text{h.c.} \right), \quad (22)$$

$$\hat{G}_2 = \sum_{j=1}^\nu \hat{c}_{j,\uparrow}^\dagger \hat{c}_{j,\uparrow} \hat{c}_{j,\downarrow}^\dagger \hat{c}_{j,\downarrow}. \quad (23)$$

All results presented for the Fermi-Hubbard model are calculated via DMRG and scaled to the thermodynamic limit. We keep a truncated bond dimension of up to $m = 1000$, and scale our results to the $m \rightarrow \infty$ limit using the variance in the internal energy.

The Bose-Hubbard model is given by

$$\hat{H}_0 = -t \sum_{j=1}^\nu \left(\hat{b}_j^\dagger \hat{b}_{j+1} + \text{h.c.} \right), \quad (24)$$

$$\hat{G}_2 = \sum_{j=1}^\nu \hat{b}_j^\dagger \hat{b}_j \hat{b}_j^\dagger \hat{b}_j, \quad (25)$$

where $\hat{b}_j^{(\dagger)}$ annihilates (creates) a boson on site j . All results for the Bose-Hubbard model are calculated via DMRG for 100 lattice sites with a bond dimension of $m = 100$. The bond dimension, which controls the accuracy of the numerical results, can be much lower than in the Fermi-Hubbard model due to the lower degree of entanglement in the Bose-Hubbard model.

Transverse field Ising model

The transverse field Ising model is given by

$$\hat{H}_0 = h_x \sum_{j=1}^{\nu} \hat{S}_j^x, \quad (26)$$

$$\hat{G}_2 = \sum_{j=1}^{\nu-1} \hat{S}_j^z \hat{S}_{j+1}^z. \quad (27)$$

We calculate the finite-temperature thermal equilibrium state of the transverse Ising model using the ancilla approach to DMRG [51]. We start from an infinite temperature state which is maximally entangled between the physical sites and ancilla states, and evolve in imaginary time using time evolving block decimation and a second order Trotter gate decomposition [51]. To avoid numerical errors in the heat capacity (Fig. 2f), arising from calculating higher order numerical derivatives at small time steps, we employ a Savitzky-Golay filter to smooth \overline{G}_2 at low temperatures [52].

The derivative of $(\partial \overline{G}_2 / \partial h_z)$, shown in the inset of Fig. 2e, cannot be directly calculated for the transverse Ising model due to the \mathcal{Z}_2 symmetry ($S_j^z \rightarrow -S_j^z$) of \overline{G}_2 . Thus, we explicitly break this symmetry by introducing a longitudinal field, i.e., adding a term $h_z \sum_{j=1}^{\nu} \hat{S}_j^z$ to Hamiltonian (26), and numerically evaluate $\partial \overline{G}_2 / \partial h_z = \lim_{h_z \rightarrow 0} [\partial \overline{G}_2(h_z) / \partial h_z]$.

Data availability

All data presented here will be made available upon publication.

Acknowledgments

We acknowledge the stimulating and insightful discussions with I. Bloch, P. Jacobson and L. Pollet. This work was supported through Australian Research Council Discovery Project Grant Nos. DP190101515, DP230100139 and DP240101033.

Author contributions

All authors contributed to the development of the method. F.R. and R.S.W. carried out and analysed the calculations for fermionic/spin and bosonic models, respectively. H.L.N., B.J.P. and K.V.K. directed the research. B.J.P. and K.V.K. conceived and planned the research.

Competing interests

The authors declare no competing interests.

Additional information

Supplementary Information Supplementary Information is available for this paper.

Correspondence and requests for materials should be addressed to B. J. Powell or K. V. Kheruntsyan.

SUPPLEMENTARY INFORMATION

S1. Thermodynamic potentials and identities for Maxwell relations involving correlations

In this section we derive generalised Maxwell relations for systems with arbitrary two-body interactions without resorting to the Hellmann-Feynman theorem. We first note that the integrated correlation function, \overline{G}_2 , is an *extensive* thermodynamic parameter that characterizes the variation of the internal energy of the system, $U = \langle \hat{H} \rangle$, with the interaction strength c , which is an *intensive* parameter conjugate to \overline{G}_2 . The extensivity of \overline{G}_2 follows immediately from the fact that $c\overline{G}_2$ is simply the expectation value of the interaction part of the Hamiltonian, $\langle \hat{H}_{\text{int}} \rangle = c \langle \overline{G}_2 \rangle$, which itself must be extensive because the overall Hamiltonian energy and the kinetic energy part alone are also extensive. For example, for a uniform 1D Lieb-Liniger gas this can also be seen explicitly as $\overline{G}_2 = \mathcal{V} \langle \hat{\Psi}^\dagger \hat{\Psi}^\dagger \hat{\Psi} \hat{\Psi} \rangle = \mathcal{V} n^2 g^{(2)}$, where \mathcal{V} is extensive, whereas n and $g^{(2)}$ are intensive.

Next, we make the dependence of the free energy on c explicit, $F = F(T, \mathcal{V}, N, c, \dots)$. Accordingly, the variation of the generalised Helmholtz free energy can be written as

$$dF = -SdT - Pd\mathcal{V} + \mu dN + \overline{G}_2 dc + \dots, \quad (\text{S1})$$

where $\mu = (\partial F / \partial N)_{T, \mathcal{V}, c}$ is the chemical potential, and $\overline{G}_2 = (\partial F / \partial c)_{T, \mathcal{V}, N}$ which we note agrees with equation (17) except that now it is derived without relying on the Hellmann-Feynman theorem. From equation (S1), one can derive all Maxwell relations as usual.

S2. Explicit integral forms of generalised Maxwell relations

In table S1, we summarise the explicit integral forms, Eqs. (6) and (8), of generalized Maxwell relations presented in Table I.

S3. Other thermodynamic ensembles

According to the standard formalism of thermodynamics (see, e.g., [21, 53]), the fundamental equation (S1) itself can be obtained from the Euler equation for the generalised internal energy of the system,

$$U(S, \mathcal{V}, N, \overline{G}_2, \dots) = TS - P\mathcal{V} + \mu N - c\overline{G}_2 + \dots, \quad (\text{S2})$$

which is a function of only extensive parameters, by means of the following Legendre transform:

$$F = U - TS + c\overline{G}_2. \quad (\text{S3})$$

The differential of U is given by

$$dU = TdS - Pd\mathcal{V} + \mu dN - c d\overline{G}_2, \quad (\text{S4})$$

TABLE S1. Integral forms of the generalised Maxwell relations involving the pair correlation \overline{G}_2 .

Thermodynamic quantity	Integral form of the Maxwell relation for \overline{G}_2
Pressure	$P(c) = P(c_0) - \int_{c_0}^c \left(\frac{\partial \overline{G}_2(c')}{\partial \mathcal{V}} \right)_{c', T, N} dc'$
Entropy	$S(c) = S(c_0) - \int_{c_0}^c \left(\frac{\partial \overline{G}_2(c')}{\partial T} \right)_{c', \mathcal{V}, N} dc'$
Chemical potential	$\mu(c) = \mu(c_0) + \int_{c_0}^c \left(\frac{\partial \overline{G}_2(c')}{\partial N} \right)_{c', T, \mathcal{V}} dc'$
Magnetization	$\mathbf{m}(c) = \mathbf{m}(c_0) - \int_{c_0}^c \nabla_{\mathbf{h}} \overline{G}_2(c') dc'$
Heat capacity	$C_{\mathcal{V}}(c) = C_{\mathcal{V}}(c_0) - T \int_{c_0}^c \left(\frac{\partial^2 \overline{G}_2(c')}{\partial T^2} \right)_{c', \mathcal{V}, N} dc'$
Isothermal compressibility	$\kappa_T^{-1}(c) = \kappa_T^{-1}(c_0) + \mathcal{V} \int_{c_0}^c \left(\frac{\partial^2 \overline{G}_2(c')}{\partial T^2} \right)_{c', T, N} dc'$

where $T = (\partial U / \partial S)_{\mathcal{V}, N, \overline{G}_2}$, $P = -(\partial U / \partial \mathcal{V})_{S, N, \overline{G}_2}$, $\mu = (\partial U / \partial N)_{S, \mathcal{V}, \overline{G}_2}$, and $c = -(\partial U / \partial \overline{G}_2)_{S, \mathcal{V}, N} = T (\partial S / \partial \overline{G}_2)_{U, \mathcal{V}, N}$. Equations (S3) and (S4) lead directly to (S1).

An equation similar to Eq. (S1) can be written for the grand-canonical thermodynamic potential $\Omega = F - \mu N$,

$$d\Omega = -SdT - Pd\mathcal{V} - Nd\mu + \overline{G}_2 dc + \dots, \quad (\text{S5})$$

with $\Omega = \Omega(T, \mathcal{V}, \mu, c, \dots)$. If there are no additional relevant parameters (represented by the ellipsis) then for homogeneous systems $\Omega = -P\mathcal{V}$ and equation (S5) can be further simplified to

$$\mathcal{V}dP - SdT - Nd\mu + \overline{G}_2 dc = 0, \quad (\text{S6})$$

which takes the role of the generalised Gibbs-Duhem relation. The generalised Gibbs-Duhem relation implies that among the four intensive parameters $\{P, T, \mu, c\}$ only three are independent, and hence the dependence of the fourth parameter on the other three takes the role of the thermodynamic equation of state, such as $P = P(T, \mu, c)$. For explicit examples of such equations of state for the uniform 1D Bose gas, see a recent review in Ref. [28].

S4. Inverse of isothermal compressibility for the Lieb-Liniger model ($Y = \kappa_T^{-1} / \mathcal{V}$, $X = X' = \mathcal{V}$)

The inverse of isothermal compressibility, $\kappa_T = -\mathcal{V}^{-1} (\partial \mathcal{V} / \partial P)_{N, T, c}$, can be expressed through the Helmholtz free energy via $\kappa_T^{-1} = \mathcal{V} (\partial^2 F / \partial \mathcal{V}^2)_{T, N, c}$, and therefore the generic equation (7) leads to the Maxwell relation given as Eq. (14) in Table I.

We evaluate κ_T^{-1} , using Eqs. (8) and (14), for the strongly interacting ($\gamma > 1$) Lieb-Liniger model at $T = 0$, where \overline{G}_2 is

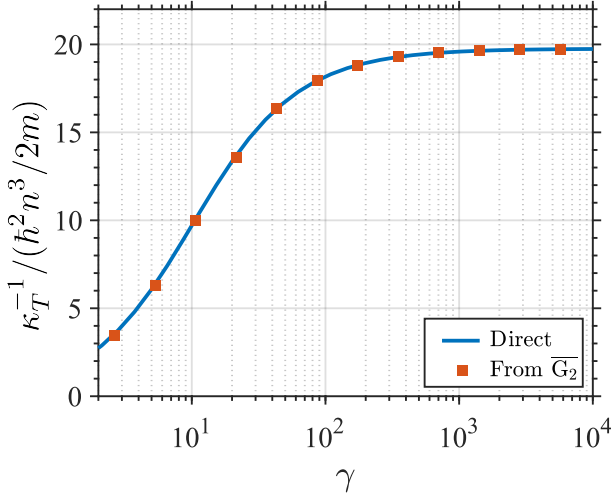


FIG. S1. Inverse isothermal compressibility (κ_T^{-1}) of the Lieb-Liniger model at $T = 0$ K in the strongly interacting regime ($\gamma > 1$). Calculations obtained directly and from numerical \overline{G}_2 are achieved using the Bethe ansatz state solutions for the ground state [26], which are exact.

calculated using the Hellmann-Feynman theorem [48]. This is in excellent agreement with direct calculation of κ_T^{-1} from the ground state energy using the Bethe ansatz [26], Fig. S1.

S5. Entropy for the Yang-Gaudin model ($Y \equiv -S, X \equiv T$)

The entropy in the canonical ensemble is defined via $S = -(\partial F/\partial T)_{V,N,c}$ and therefore the generalised Maxwell relation between S and \overline{G}_2 acquires the form of Eq. (10), Table I.

To illustrate the utility of this Maxwell relation in the Yang-Gaudin model [34, 35, 50], we utilise the known approximate analytic expressions for the normalised local pair correlation function [54],

$$g_{\uparrow\downarrow}^{(2)}(0) = 4 \frac{\langle \hat{\Psi}_{\uparrow}^{\dagger}(x) \hat{\Psi}_{\downarrow}^{\dagger}(x) \hat{\Psi}_{\downarrow}(x) \hat{\Psi}_{\uparrow}(x) \rangle}{n^2} \quad (\text{S7})$$

$$= (1 - \mathcal{P}^2) \frac{\langle \hat{\Psi}_{\uparrow}^{\dagger}(x) \hat{\Psi}_{\downarrow}^{\dagger}(x) \hat{\Psi}_{\downarrow}(x) \hat{\Psi}_{\uparrow}(x) \rangle}{n_{\uparrow} n_{\downarrow}}, \quad (\text{S8})$$

where $n = n_{\uparrow} + n_{\downarrow}$ is the total uniform density, $n_{\uparrow(\downarrow)} = \langle \hat{\Psi}_{\uparrow(\downarrow)}^{\dagger}(x) \hat{\Psi}_{\uparrow(\downarrow)}(x) \rangle$ is the density in the spin up (down) component, and $\mathcal{P} = (n_{\uparrow} - n_{\downarrow})/n$ is the polarisation. The local pair correlation $g_{\uparrow\downarrow}^{(2)}(0)$ can be found through a relation with Tan's contact parameter \mathcal{C} , namely $g_{\uparrow\downarrow}^{(2)}(0) = (4/c^2 n^2) \mathcal{C}$ [55–57] and hence $\overline{G}_2 = (4V/c^2 n^2) \mathcal{C}$, and the known result for \mathcal{C} itself [54, 58].

At sufficiently high temperatures, $k_B T \gg \hbar^2 c^2 / 2m$, these

results allow us to express $g_{\uparrow\downarrow}^{(2)}(0)$ as

$$g_{\uparrow\downarrow}^{(2)}(0) = (1 - \mathcal{P}^2) \left\{ 1 - \frac{\sqrt{\pi} \gamma}{\sqrt{2\tau}} e^{\frac{\gamma^2}{2\tau}} \left[1 - \operatorname{erf} \left(\frac{\gamma}{\sqrt{2\tau}} \right) \right] \right\}, \quad (\text{S9})$$

where we have introduced a dimensionless interaction strength $\gamma = 2cm/\hbar^2 n$ for constant total density n , and a dimensionless temperature $\tau = 2mk_B T/\hbar^2 n^2$. Simplifying this expression further using the lowest order Taylor expansion (such that the resulting entropy may be compared with the similar analytic result derived in Ref. [23] for the Lieb-Liniger model), we then use Eqs. (6) and (10) to obtain:

$$S \simeq S_{\text{IFG}} - \frac{N(1 - \mathcal{P}^2)}{16\hbar} \sqrt{\frac{\pi m}{2k_B T^3}} n c^2. \quad (\text{S10})$$

Here, $S_{\text{IFG}} \equiv S(c = 0)$ is the entropy of an ideal Fermi gas (see, e.g., Ref. [28]). To the best of our knowledge, this approximate analytic result for the entropy of the Yang-Gaudin model has not been derived before.

S6. Exact calculation of the magnetization of the transverse field Ising model at $T = 0$

The spin-spin correlation functions for the transverse field Ising model have been extensively studied, with the nearest neighbour longitudinal spin-spin correlation given by [42]

$$\overline{G}_2 = \frac{1}{4\pi} \int_0^{\pi} dk \Lambda_k^{-1} \cos(k) + \frac{c}{8h_x \pi} \int_0^{\pi} dk \Lambda_k^{-1}, \quad (\text{S11})$$

where Λ_k is the energy of the non-interacting fermions after a Jordan-Wigner transformation is performed, given by

$$\Lambda_k = \sqrt{1 + \left(\frac{c}{h_x} \right)^2 + \frac{c \cos(k)}{h_x}}. \quad (\text{S12})$$

The derivative of equation (S11) with respect to h_x is given by

$$\frac{\partial \overline{G}_2}{\partial h_x} = \frac{1}{4\pi} \int_0^{\pi} dk \frac{\partial \Lambda_k^{-1}}{\partial h_x} \left(\cos(k) + \frac{c}{h_x} \right) + \frac{c}{8h_x^2 \pi} \int_0^{\pi} dk \Lambda_k^{-1}. \quad (\text{S13})$$

Combining Eq. (S13) with Eqs. (6) and (12) of the main text allows the transverse magnetization at zero temperature to be calculated, Fig. 2d.

S7. Scaling of $\partial \overline{G}_2 / \partial h_x$ near the quantum critical point of the transverse field Ising model

Evaluating $\partial \overline{G}_2 / \partial h_x$ to measure the longitudinal magnetization, m^z , for the Ising model, results in a ‘lambda’ anomaly

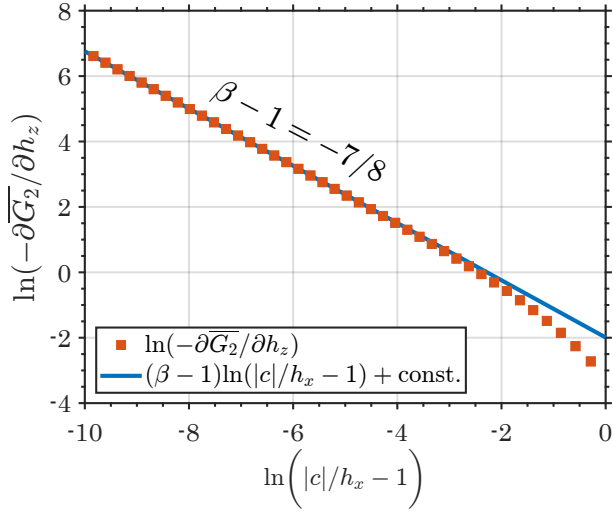


FIG. S2. Zero temperature $\partial\overline{G}_2/\partial h_x$ displays scaling behaviour near the critical point of the transverse field Ising model. Linear regression reveals the scaling law behaviour follows $-\partial\overline{G}_2/\partial h_x \propto [|c|/h_x - 1]^{\beta-1}$ where $\beta = 1/8$ is the order parameter critical exponent. $\partial\overline{G}_2/\partial h_x$ is calculated exactly using Eq. (S14).

as shown in the inset of Fig. 2e. As the longitudinal magnetization serves as the order parameter in this model, the order parameter critical exponent, β , can be extracted from $\partial\overline{G}_2/\partial h_z$ close to the critical point.

The longitudinal magnetization for the transverse Ising model is analytically given by $m_z = (1 - (|c|/h_x)^{-2})^\beta$ [42]. Using the Maxwell relation given by Eq. (12), $-\partial\overline{G}_2/\partial h_z = \partial m_z/\partial c$, it can be shown that $\ln(-\partial\overline{G}_2/\partial h_z)$ is exactly given by

$$\ln\left(-\frac{\partial\overline{G}_2}{\partial h_x}\right) = -3\ln(|c|/h_x) - \ln(4) + (\beta - 1)\ln\left(1 - (|c|/h_x)^{-2}\right). \quad (\text{S14})$$

Near the critical point ($|c| = h_x$) we have $\lim_{|c|/h_x \rightarrow 1} \ln(|c|/h_x) = 0$ and $1 - (|c|/h_x)^{-2} \simeq 2(|c|/h_x - 1)$; hence the critical exponent can then be extracted from a log-log plot of $\partial\overline{G}_2/\partial h_z$. This is illustrated in Fig. S2, where, as the critical point is approached, $\partial\overline{G}_2/\partial h_z$ displays linear scaling behaviour and the critical exponent can be extracted. We find excellent agreement with the textbook result $\beta = 1/8$ [40, 42].